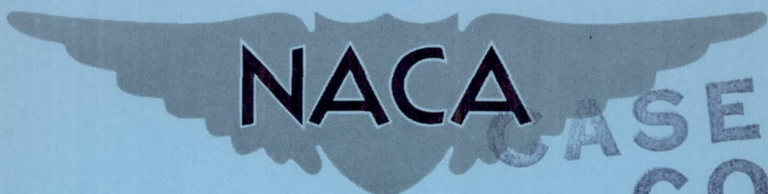


**CONFIDENTIAL**

NACA RM A55D06



**CASE FILE  
COPY**

# RESEARCH MEMORANDUM

A METHOD FOR EVALUATING THE LOADS AND CONTROLLABILITY

ASPECTS OF THE PITCH-UP PROBLEM

By Melvin Sadoff, Frederick H. Matteson,  
and C. Dewey Havill

Ames Aeronautical Laboratory  
Moffett Field, Calif.

**CLASSIFICATION CHANGED TO UNCLASSIFIED  
AUTHORITY: NASA TECHNICAL PUBLICATIONS  
ANNOUNCEMENT NO. 8  
EFFECTIVE DATE: JULY 22, 1959**

WHL

CLASSIFIED DOCUMENT

This material contains information affecting the National Defense of the United States within the meaning of the espionage laws, Title 18, U.S.C., Secs. 793 and 794, the transmission or revelation of which in any manner to an unauthorized person is prohibited by law.

## NATIONAL ADVISORY COMMITTEE FOR AERONAUTICS

WASHINGTON

August 23, 1955

**CONFIDENTIAL**

## NATIONAL ADVISORY COMMITTEE FOR AERONAUTICS

RESEARCH MEMORANDUM

## A METHOD FOR EVALUATING THE LOADS AND CONTROLLABILITY

## ASPECTS OF THE PITCH-UP PROBLEM

By Melvin Sadoff, Frederick H. Matteson,  
and C. Dewey Havill

## SUMMARY

A procedure is described for estimating the range of peak airplane load factors and maneuvering tail loads likely to be experienced in pitch-up maneuvers. The method assumes a realistic evaluation maneuver which partially integrates airplane and pilot response.

Results of computations, in which it is assumed that this evaluation maneuver is used on an example swept-wing airplane at 35,000 and 15,200 feet, indicated that though the load factors and maneuvering tail loads were not critical in pitch-up maneuvers at 35,000 feet, they were likely to exceed design levels at 15,200 feet. It was shown, however, that for corrective-control rates of  $45^\circ$  per second or higher, the airplane load factors would not exceed the design value by more than 10 percent. It was indicated that it would be desirable to restrict the maximum available corrective-control rate to some optimum value which compromises the high rates required to minimize overshoot load factor with the low rates desirable for low maneuvering tail loads.

A tentative criterion, based on the ratio of the destabilizing moment at the time of corrective-control application to the corrective-control moment per unit stick deflection available to the pilot, appears promising for predicting controllability of pitch-up. Preliminary information on two swept-wing fighter airplanes indicated that ratios of 1 to 20 and 1 to 100 were associated with an uncontrollable pitch-up and a relatively controllable pitch-up, respectively.

## INTRODUCTION

One of the important problems experienced with swept-wing airplanes is the undesirable pitch-up tendency associated with nonlinear pitching-moment curves. The pitch-up is considered undesirable in two main

respects. Under certain conditions, the design wing and horizontal-tail loads may be exceeded inadvertently in pitch-up maneuvers. Furthermore, the occurrence of pitch-up limits controlled maneuvering, in many cases, to load factors below the pitch-up boundary; in others, it results in a significant reduction in controllability.

Several flight investigations (refs. 1 to 4) and an analytical study (ref. 5) provide some information of general interest in connection with the loads and controllability aspects of the pitch-up problem. Reference 1 presents some experimental evidence of the possibility of encountering large wing and tail loads in pitch-up maneuvers. In references 2 to 4, pilot opinion of the pitch-up characteristics and controllability of two  $35^\circ$  swept-wing airplanes with various wing and tail modifications is presented. The analytical investigation of reference 5 assesses various pitching-moment irregularities in terms of the abruptness of the airplane response during pitch-up to a more or less arbitrary control input; however, no specific attempt was made to consider quantitatively the load factors and tail loads or the relative controllability that may be expected in specified pitch-up maneuvers.

The purpose of the present paper is to outline a procedure, based on an assumed realistic control input (or evaluation maneuver), which may be used to assess primarily the loads aspects of the pitch-up problem. Also, the possibility of predicting the degree of controllability of a specified pitch-up tendency is briefly discussed. Computations are made for an example swept-wing fighter airplane to illustrate the use of the method.

#### NOTATION

- $b$  airplane damping coefficient,  $\frac{-Z_{\dot{\alpha}}}{mV} - \frac{M_{\dot{\alpha}} + M_{\dot{\theta}}}{I_y}$ , 1/sec
- $C_0$  control-deflection coefficient,  $\frac{M_{\delta_e}}{I_y} - \frac{M_{\theta} Z_{\delta_e}}{I_y mV}$ , 1/sec<sup>2</sup>
- $C_1$  control-rate coefficient,  $\frac{Z_{\delta_e}}{mV}$ , 1/sec
- $C_m$  airplane pitching-moment coefficient about airplane center of gravity,  $\frac{\text{airplane pitching moment}}{qS\bar{c}}$
- $C_L$  airplane lift coefficient,  $\frac{L}{qS}$

- $C_N$  airplane normal-force coefficient,  $\frac{N}{qS}$
- $\bar{c}$  wing mean aerodynamic chord, ft
- $g$  acceleration of gravity,  $1 g = 32.2 \text{ ft/sec}^2$
- $h_p$  pressure altitude, ft
- $I_y$  airplane pitching moment of inertia, slug-ft<sup>2</sup>
- $K$  parameter denoting damping ratio of airplane to that of horizontal tail
- $k$  airplane spring constant,  $\frac{-M_{\alpha}}{I_y} + \frac{Z_{\alpha} M_{\dot{\theta}}}{I_y m V}$ ,  $1/\text{sec}^2$
- $l_t$  distance from airplane center of gravity to aerodynamic center of horizontal tail, ft
- $L$  airplane lift, lb
- $L_t$  horizontal-tail lift, lb
- $\Delta M_0$  intercept of a particular linear segment of the pitching-moment curve on the ordinate axis,  $\Delta \alpha = 0$
- $m$  airplane mass,  $\frac{W}{g}$ , slugs
- $N$  airplane normal force, lb
- $n$  airplane normal load factor,  $\frac{N}{W}$
- $q$  dynamic pressure, lbs/sq ft

S	wing area, sq ft
$S_t$	horizontal-tail area, sq ft
s	variable introduced in Laplace transform
t	time, sec
V	airplane velocity, ft/sec
W	airplane weight, lb
$\alpha$	airplane angle of attack, deg or radians
$\gamma$	flight-path angle, radians
$\delta_e$	elevator angle, deg or radians
$\delta_{stick}$	control-stick angle (fore and aft), radians from neutral
$\Delta$	when preceding symbol denotes increment from steady-state condition
$\epsilon$	downwash angle, deg or radians
$\eta_t$	horizontal-tail efficiency factor, $\frac{q_t}{q}$
$\theta$	angle of pitch, radians
$\rho$	mass density of air, slugs/cu ft
$C_{L_\alpha}$	airplane lift-curve slope, $\frac{dC_L}{d\alpha}$ , 1/radian

$(C_{L\alpha})_t$  horizontal-tail lift-curve slope,  $\frac{dC_{L_t}}{d\alpha_t}$ , 1/radian

$C_{L\delta_e}$   $\frac{dC_L}{d\delta_e}$ , 1/radian

$C_{m\alpha}$   $\frac{dC_m}{d\alpha}$ , 1/radian

$C_{m\delta_e}$   $\frac{dC_m}{d\delta_e}$ , 1/radian

$M_{\alpha}$   $(C_{m\alpha})qS\bar{c}$ , ft-lb/radian

$M_{\dot{\alpha}}$   $M_{\dot{\theta}_t} \left( \frac{\partial \epsilon}{\partial \alpha} \right)$ ,  $\frac{\text{ft-lb}}{\text{radian/sec}}$

$M_{\delta_e}$   $(C_{m\delta_e})qS\bar{c}$ , ft-lb/radian

$M_{\delta_{\text{stick}}}$   $(C_{m\delta_{\text{stick}}})qS\bar{c}$ , ft-lb/radian

$M_{\dot{\theta}_t}$   $\frac{-\eta_t (C_{L\alpha})_t \rho V S_t l_t^2}{2}$ ,  $\frac{\text{ft-lb}}{\text{radian/sec}}$

$M_{\dot{\theta}}$   $K M_{\dot{\theta}_t}$ ,  $\frac{\text{ft-lb}}{\text{radian/sec}}$

$Z_{\alpha}$   $-[(C_{L\alpha})qS]$ , lb/radian

$Z_{\delta_e}$   $-[(C_{L\delta_e})qS]$ , lb/radian

$\left. \begin{matrix} \dot{\alpha}, \dot{\gamma}, \dot{\delta}_e, \\ \dot{\theta}, \dot{n} \end{matrix} \right\}$  equivalent notation for  $\frac{d\alpha}{dt}$ ,  $\frac{d\gamma}{dt}$ ,  $\frac{d\delta_e}{dt}$ ,  $\frac{d\theta}{dt}$ , and  $\frac{dn}{dt}$

$\ddot{\alpha}, \ddot{\gamma}, \ddot{\theta}$  equivalent notation for  $\frac{d^2\alpha}{dt^2}$ ,  $\frac{d^2\gamma}{dt^2}$ , and  $\frac{d^2\theta}{dt^2}$

## Subscripts

t	horizontal tail
$\ddot{\theta}$	corresponding to a specified value of pitching acceleration
i	initial conditions in ith time interval
max	maximum value
th	threshold
D	duration of pitching-acceleration stimulus

## DESCRIPTION OF EXAMPLE AIRPLANE

The example airplane used in the present computations is a jet-powered swept-wing fighter type. A photograph of the airplane is presented in figure 1, and the physical characteristics and a two-view drawing of the airplane are given in table I and figure 2, respectively.

## DESCRIPTION OF METHOD

## Evaluation Maneuver

A realistic evaluation of the loads that might occur during a pitch-up requires the establishment of a rational pitch-up evaluation maneuver. In general, a pitch-up maneuver may be expected to consist of three distinct parts: (1) application of elevator control at a constant rate until the pilot detects pitch-up; (2) continued application of control at the initial rate for an interval depending on the pilot's reaction time; and (3) application of corrective control to arrest the pitch-up at a rate depending on several factors including pilot experience with pitch-up, intensity of pitch-up, and proximity to the design load factor.

It is necessary in order to arrive at a rational evaluation maneuver to identify and determine the level of a response quantity which the pilot associates with the onset of pitch-up. It is also necessary to determine a reasonable average pilot reaction time. Some limited results in references 2 and 3 indicated that an appropriate response quantity might be pitching acceleration, since the pilots appeared to associate different levels of pitch-up intensity with the magnitude of pitching acceleration developed during pitch-up. In view of this, tests were conducted on a modified Link trainer, to ascertain whether there existed a minimum value

of pitching acceleration which correlated consistently with the pilots' initial appreciation of pitch-up. The results of these tests, which are described in more detail in Appendix A, indicated a fairly consistent correlation of a pitching acceleration threshold  $\Delta\ddot{\theta}$  of about 0.15 with the pilots' initial perception of pitch-up. The tests also indicated a mean reaction time of about 0.3 second. For the present analysis, an additional 0.1 second (or a total of 0.4 second) was applied to account for the time required to accelerate the control surface from rest to a constant rate.

With the concept of a pitching-acceleration threshold established, and a reasonable reaction time, and with the pertinent aerodynamic and geometric data known, it was then possible to define parts (1) and (2) of the evaluation maneuver. Since it was not possible to predict the exact control rate used by a pilot to arrest a specified pitch-up tendency, a range of corrective-control rates was selected for part (3) of the evaluation maneuver to illustrate the effect of this variable on the load factors and tail loads that may be experienced in pitch-up maneuvers.

The control inputs, established by the above procedure for the example airplane, are presented in figure 3 for a Mach number of 0.90 (the speed at which the pitch-up is most severe for the example airplane) and for two altitudes - 35,000 feet and about 15,000 feet. The upper altitude was chosen to correspond to the altitude at which most of the flight tests were performed on the example airplane and the lower altitude was selected to illustrate the loads aspects of the pitch-up problem at low altitude. In the present example, this altitude corresponds to the altitude at which the pitch-up flight region (lower boundary defined herein as the angle of attack for neutral stick-fixed stability) was just penetrated in a 6 g maneuver. The several initial control rates (fig. 3), which correspond to initial values of  $\dot{n}$  of 0.2, 0.5, and 1.0 g per second, were selected to cover a reasonable range of entry rates from the relatively gradual maneuvers used by Ames pilots in research tests to the more abrupt maneuvers that are likely to be used in training or combat.

### Computational Procedure

The equations of motion and the pertinent aerodynamic and geometric data used in the computations are presented in Appendix B. Airplane responses associated with the elevator motions shown in figure 3 were obtained with a Reeves Electronic Analog Computer.

In the event that an analog computer is not readily available, or where there are only a few configurations to check, a computational procedure using the Laplace transform method is also described in Appendix B. A sample set of computations is presented and the results are compared with the solutions obtained from the REAC.



APPLICATION OF METHOD TO EXAMPLE  
SWEPT-WING FIGHTER AIRPLANE

Loads

Computed response quantities for the example airplane at 35,000 feet are presented in figure 4. Incremental angle-of-attack and pitching-acceleration variations are shown in figure 4(a), while computed time histories of airplane load factor and incremental maneuvering horizontal-tail load are given in figure 4(b). The dashed lines in figures 4(a) and 4(b) marked "limit of  $\Delta C_m(\alpha)$  and  $\Delta C_N(\alpha)$  curves" refer to the maximum values of  $\Delta\alpha$  and  $n$  for which experimental pitching-moment and lift data used in the computations were available. The two vertical ticks on the  $\Delta\alpha$  and  $n$  responses indicate, respectively, the time at which the pilot would first perceive pitch-up ( $\Delta\ddot{\theta} = 0.15$ ) and the time at which corrective control was initiated. The results in figure 4 indicate that for corrective-control rates of  $20^\circ$  per second or less, recovery does not generally occur within the angle-of-attack range for which the computations are available, and the overshoot<sup>1</sup> values of  $\Delta\alpha$  and  $n$  are relatively large, exceeding  $9^\circ$  and 2.5, respectively. For the higher corrective-control rates, recovery occurs at incremental angles of attack of less than  $8^\circ$  and at load factors less than 4, and the overshoot in angle of attack and load factor is about  $3.5^\circ$  and 1.5, respectively. There does not appear to be any consistent effect of entry rate  $\dot{n}$  on the peak airplane responses during pitch-up (fig. 4). However, it may be pointed out that for a constant corrective-control rate, the overshoot values of angle of attack and load factor increase appreciably with an increase in entry rate. It should also be noted that the values of  $\Delta\alpha$  and  $n$  at the pitching-acceleration threshold decrease appreciably with an increase in entry rate. The results in figure 4 also show little variation of the peak negative pitching acceleration or maximum positive incremental maneuvering tail load with entry rate  $\dot{n}$ . In the present example, the peak values of  $\ddot{\theta}$  and  $\Delta L_{t_{\theta}}$  for corrective-control rates above  $20^\circ$  per second are limited by the maximum down-elevator deflection available.

Figure 5 presents computed response quantities for the example airplane in pitch-up maneuvers at 15,200 feet. Incremental angle-of-attack and pitching-acceleration time histories are presented in figure 5(a), and normal load factor and incremental maneuvering horizontal-tail load variations are shown in figure 5(b). Comparison of these results with those of figure 4 indicates that for the same values of corrective-control rate and entry rate, the overshoot in angle of attack at the lower altitude is only about 60 percent of that at 35,000 feet. In the present case, this results

---

<sup>1</sup>In the present analysis, overshoot is defined as the difference between the peak values of  $\Delta\alpha$  and  $n$  and the values existing at the time the threshold value of pitching acceleration was attained.

---

in overshoot load factors at 15,200 feet about 50 percent greater than those at 35,000 feet. It may be noted that the peak load factors reached in the assumed pitch-up maneuvers at 15,200 feet exceed the design value appreciably for the lower corrective-control rates. However, for corrective-control application at a rate of  $45^\circ$  per second or higher, the value of  $n_{\max}$  would not exceed the design level by more than 10 percent. For the same corrective-control rates, the peak negative pitching accelerations and the corresponding maximum incremental tail loads attained in pitch-up maneuvers at 15,200 feet (fig. 5) are approximately 50 to 100 percent greater than the peak values reached at 35,000 feet (fig. 4). The results in figure 5(b) show, for a constant corrective-control rate, relatively small difference in  $\Delta L_{t_{\dot{\theta}_{\max}}}$  due to changes in entry rate  $\dot{n}$ ,

while a substantial increase in tail load is associated with an increase in corrective-control rate. These and the foregoing results suggest that it may be desirable to limit the maximum available control rate to some optimum value which compromises a reduction in overshoot load factor with a decrease in the maneuvering tail load.

Summary plots, which may be useful in selecting an optimum control rate, are presented in figures 6 and 7 for altitudes of 35,000 and 15,200 feet, respectively. Values of overshoot load factor and incremental maneuvering horizontal-tail load are plotted as a function of corrective-control rate for various values of  $\dot{n}$ . The results at 35,000 feet (fig. 6) indicate that for corrective-control rates above  $45^\circ$  per second, only a small further reduction in overshoot load factor occurs, while practically no change occurs in the values of  $\Delta L_{t_{\dot{\theta}_{\max}}}$ . At 15,200 feet (fig. 7), for corrective-control rates greater than about  $45^\circ$  per second and up to the maximum rate considered of  $75^\circ$  per second, the overshoot load factor is further reduced by only approximately 0.2 (3 percent of the design value), while the values of  $\Delta L_{t_{\dot{\theta}_{\max}}}$  increase from roughly 90 percent to 120 percent of the design tail load for the example airplane. It appears, on the basis of these results, that it might be desirable to limit the maximum available control rate to about  $45^\circ$  per second, since a further increase in rate results in an appreciable increase in maneuvering tail load without materially reducing the overshoot load factor.

### Controllability

In a previous flight study of the pitch-up problem on the example airplane (ref. 2), it was indicated that pilot opinion of the pitch-up appeared related to the level of peak positive pitching acceleration experienced during the pitch-up maneuvers. Although the magnitude of the peak pitching-acceleration response may describe the relative controllability of a pitch-up tendency on a given airplane, where the effectiveness

of several modifications on the pitch-up is being evaluated (as in ref. 2, for example), this response quantity alone is not sufficient to indicate the relative controllability of pitch-up on several different airplanes with different pitching moments of inertia and longitudinal control effectiveness. In a preliminary assessment of the problem, it was decided that a more general controllability criterion might comprise all three of these quantities, that is, pitching acceleration, moment of inertia, and control effectiveness, and would relate the unstable pitch-up moment  $I_y \ddot{\theta}_{\max}$  at the time of corrective-control application to the corrective-control moment per unit stick deflection available to the pilot  $M_{\delta_{\text{stick}}}$ .

A plot presenting the variation of the controllability parameter  $I_y \ddot{\theta} / M_{\delta_{\text{stick}}}$  with entry rate  $\dot{n}$  is shown in figure 8 for the example airplane at 35,000 and 15,200 feet. It may be noted that an increase in value of this parameter implies a decrease in controllability of the associated pitch-up tendency. The results in figure 8 indicate a significant reduction in controllability with an increase in entry rate  $\dot{n}$  for both 35,000 and 15,200 feet. It also appears from the results in figure 8 that the pitch-up for the example airplane is more easily controlled at 15,200 feet than at 35,000 feet, since the corrective-control moment per unit stick deflection  $M_{\delta_{\text{stick}}}$  increases more rapidly than the destabilizing moment  $I_y \ddot{\theta}_{\max}$  with a decrease in altitude.<sup>2</sup>

Flight tests at 0.90 Mach number at 35,000 feet, where entry rates  $\dot{n}$  of 0.2 g per second to 0.5 g per second were used to enter the pitch-up region, have indicated that the pitch-up tendency on the unmodified example airplane was relatively uncontrollable. From the upper curve in figure 8, it may be noted that the computed values of controllability factor corresponding to this uncontrollable pitch-up vary between about 0.05 and 0.065. In order to provide some information on the magnitude of the parameter  $I_y \ddot{\theta}_{\max} / M_{\delta_{\text{stick}}}$  corresponding to an airplane which has a relatively mild pitch-up and which is considered fairly controllable, computations were also made for the 35° swept-wing airplane described in

<sup>2</sup>It should be recognized, however, that since the controllability parameter  $I_y \ddot{\theta}_{\max} / M_{\delta_{\text{stick}}}$  is roughly an inverse measure of the ability of the pilot to reduce a given destabilizing moment (hence angular acceleration) to zero, the improved controllability in the present case refers only to the ability of the pilot to control airplane attitude, that is, angle of attack, angle of pitch, etc. This was touched upon previously in the discussion where it was noted the overshoot in angle of attack at 15,200 feet was only about 60 percent of that at 35,000 feet. (If it is desired to define controllability as the ability of the pilot to control load factor, then the proposed controllability parameter should be multiplied by appropriate values of dynamic pressure and lift-curve slope. The controllability parameter would then be greater at the lower altitude, i.e., a reduction in controllability. This is in agreement with the larger overshoot in load factor at the lower altitude previously noted.)

reference 4. This airplane differs from the example airplane mainly in that its pitching moment of inertia and longitudinal control effectiveness are greater than those of the example airplane by factors of  $1\frac{1}{2}$  and 4, respectively. The computed results for this airplane are shown in figure 9 where they are compared with the data for the example airplane at 35,000 feet. It may be seen that the values of the controllability parameter for the reference airplane are only about 20 percent of those for the example airplane over the range of entry rates  $\dot{n}$  covered in the computations.

It is recognized that the proposed controllability criterion should be checked for a number of airplane configurations for which pilots' opinions of the pitch-up characteristics are available. A study of this kind, directed toward prediction of pitch-up characteristics, is currently under way.

#### CONCLUSIONS

A method is described for predicting the range of airplane load factors and horizontal-tail loads that may be experienced in pitch-up maneuvers. The method is based on a realistic evaluation maneuver wherein it is assumed that the pilot applies nose-up longitudinal control at a constant rate until 0.4 second after the pitching acceleration has increased 0.15 radian per second per second above the steady-state value, at which time nose-down corrective control is applied at various constant rates. Application of the procedure to an example swept-wing fighter airplane has led to the following conclusions:

1. At 35,000 feet where the pitch-up region was entered at load factors well under the design value, the results of the analysis indicated that the airplane load factors and the incremental maneuvering horizontal-tail loads likely to be experienced in pitch-up maneuvers were not critical. The load factors would generally be restricted to values below the design level, either by the application of adequate corrective control or by the stall, while the tail loads were limited, in general, by the maximum down-elevator control available.

2. At 15,200 feet where the pitch-up region was entered in a maneuver between 5 g and 6 g, the analysis indicated both the load factors and tail loads likely to be encountered in pitch-up maneuvers would exceed design values. However, for corrective-control application at the rate of  $45^\circ$  per second or higher, the peak load factors would not exceed the design level by more than 10 percent.

3. Based on the results of the present analysis, it appears desirable to restrict the maximum control rate on airplanes which experience pitch-up to a value based on a compromise between desirable reductions in overshoot load factors and maneuvering tail loads. For the example airplane considered in the present analysis, an optimum rate of  $45^\circ$  per

second is indicated, since greater rates would result in greater tail loads without materially effecting a further reduction in overshoot load factor.

4. A computed parameter, based on the ratio of the unstable pitch-up moment at the time of corrective-control application to the corrective-control moment per unit stick deflection available to the pilot, appears promising for predicting controllability of pitch-up. Preliminary information available on two swept-wing fighter airplanes indicated that for a pitch-up considered uncontrollable by the pilots, the ratio  $I_y \ddot{\theta}_{\max} / M_{\delta_{\text{stick}}}$  is of the order of 1 to 20, while for a relatively controllable pitch-up, the ratio is about 1 to 100.

Ames Aeronautical Laboratory,  
National Advisory Committee for Aeronautics,  
Moffett Field, Calif., Apr. 6, 1955.

## APPENDIX A

## LINK TRAINER TESTS

These tests were designed to determine empirically the values of pilots' reaction time and pitching-acceleration threshold needed to construct the pitch-up evaluation maneuver used in this report. The problem is analogous to that described in several research projects directed toward defining the transfer functions of a human operator. The available literature and results are summarized in references 6 to 9. Although these references contained some results on reaction time to a pitching-acceleration stimulus and on threshold values of pitching acceleration, these data were not, in general, considered applicable to the present analysis since they were not obtained in an appropriate environment.

In order to keep the environment as close to flight as practicable the tests were made in a Link trainer modified so that an outside operator could introduce arbitrary pitching motions which were independent of those associated with operation of the control stick. The trainer, figure 10, was equipped with instruments to record stick position, pitching velocity and acceleration, and time. The procedure was to measure the reaction time separately and then to deduce the pitching-acceleration threshold from the type of run shown in figure 11. As it was not possible to measure the reaction time to a vestibular stimulus using the modified Link trainer, the reaction time to a visual stimulus was used because, in the present case, the proper environment was considered more important than the type of stimulus used.

The technique for measuring reaction time was to have the pilot make a gradual pull-out. At various random positions of the Link the operator would turn on an indicator light. The pilot was instructed to push the stick forward immediately upon seeing the light. The time interval between the light going on and the start of control application was considered the reaction time. This procedure was also used with the pilot distracted by having to hold a constant heading, with and without rough air. The test results from 20 to 30 runs each on three pilots and three engineers are summarized in table II. The mean reaction time is about 0.3 second which is in good agreement with the various data cited in reference 6.

As indicated on figure 11 the procedure in the runs to determine pitching-acceleration threshold was to have the pilot make a gradual pull-out; then at a random time and using various angular velocity and acceleration rates, the outside operator would induce a pitch-up. The pilot was instructed to recover by pushing forward on the stick as soon as he perceived a pitch-up. As previously shown the threshold pitching acceleration was determined as the value existing a fraction of a second, equal to the subject's mean visual reaction time, before the application of

corrective control. (See fig. 11.) In order to establish whether visual perception or angular position or velocity was a factor, runs were made with the pilot looking at the instrument panel with the gyro horizon covered and uncovered, with the pilot looking out through a window in the canopy, and with the pilot's eyes closed. Tests were again run with the pilot being distracted by the necessity for maintaining a constant heading with and without simulated rough air. No appreciable effect was noted due to any of these variables.

The results from 20 to 30 runs on each of three pilots and one engineer indicated a mean threshold of 0.12 radian per second as shown in table III. Since both the reaction time and threshold are statistical quantities there was a fairly large scatter indicated by the standard deviations. As shown in figure 12 the value of 0.12 radian per second per second is in general agreement with results from reference 9 which were presented as a function of the time duration of the stimulus. It may be noted that the pitching-acceleration threshold tends to decrease with an increase in the duration of the stimulus up to about 8 seconds. A limited series of flight tests (4 runs) on an F-84F airplane, which were made to check the Link data, indicated a mean value of 0.18 radian per second per second. The value used to construct the model pitch-up evaluation maneuver was selected as 0.15 radian per second per second.

## APPENDIX B

## METHODS OF COMPUTATION

## REAC Method

If a constant speed maneuver is assumed and if some of the higher order derivatives are neglected, the longitudinal equations of motion used may be written as

$$-mV\dot{\gamma} = Z(\alpha) + Z_{\delta_e}\Delta\delta_e \quad (B1)$$

$$I_y\ddot{\theta} = M(\alpha) + M_{\dot{\alpha}}\dot{\alpha} + M_{\dot{\theta}}\dot{\theta} + M_{\delta_e}\Delta\delta_e \quad (B2)$$

where the nonlinear functions  $Z(\alpha)$  and  $M(\alpha)$  were obtained from the upper two solid curves in figure 13, and the other pertinent information was obtained from tables I and IV. It may be noted that either for the sake of simplicity or because insufficient information was available to define the variations, the values of  $M_{\dot{\alpha}}$ ,  $M_{\dot{\theta}}$ , and  $M_{\delta_e}$  were assumed constant over the angle-of-attack range. Solutions were then obtained of  $\Delta\alpha(t)$ ,  $\ddot{\theta}(t)$ , and  $\dot{\gamma}(t)$  for the longitudinal control inputs shown in figure 3.

## Laplace Transform Method

In this method the nonlinear pitching-moment and lift curves are divided into several linear segments approximating the original curves, as illustrated in figure 13. Computations are then made for several time intervals where a new interval is dictated either by a change in slope of the linearized pitching-moment curve (fig. 13) or by the application of corrective control. The longitudinal equations of motion used in this case are

$$-mV\dot{\gamma} = Z_{\alpha}\Delta\alpha + Z_{\delta_e}\Delta\delta_e \quad (B3)$$

$$I_y\ddot{\theta} = M_{\alpha}\Delta\alpha + M_{\dot{\alpha}}\dot{\alpha} + M_{\dot{\theta}}\dot{\theta} + M_{\delta_e}\Delta\delta_e \quad (B4)$$

where  $Z_{\alpha}$ ,  $M_{\alpha}$ , and  $M_{\dot{\alpha}}$  are appropriate to the particular linear segment of pitching-moment curve under consideration. (See fig. 13.) The values of  $Z_{\delta_e}$ ,  $M_{\delta_e}$ , and  $M_{\dot{\theta}}$  were assumed constant over the entire range of angle



of attack. Since it is assumed that  $\dot{\gamma} = \dot{\theta} - \dot{\alpha}$ , equations (B3) and (B4) may be reduced to the equivalent second-order equation

$$\ddot{\alpha} + b\dot{\alpha} + k\alpha = C_0\Delta\delta_e + C_1\dot{\delta}_e + (\Delta M_0/I_y)_i \quad (B5)$$

where  $\Delta\delta_e = \dot{\delta}_e(t - t_i) + \Delta\delta_{e_i}$  and  $(\Delta M_0/I_y)_i$  is proportional to the intercept of the linear pitching-moment segment under consideration in the  $i$ th time interval on the ordinate axis ( $\Delta\alpha = 0$ ). The general Laplace transformation of equation (B5) neglecting the  $C_1\dot{\delta}_e$  term, which is generally small, and for a step (of magnitude  $\Delta\delta_{e_i}$ ) plus a ramp elevator motion may be expressed as

$$s^2\Delta\alpha(s) + sb\Delta\alpha(s) + k\Delta\alpha(s) - (s + b)\Delta\alpha_i - \dot{\alpha}_i = \frac{C_0\dot{\delta}_e}{s^2} + \frac{C_0\Delta\delta_{e_i} + (\Delta M_0/I_y)_i}{s}$$

from which

$$\Delta\alpha(s) = \frac{(s + b)\Delta\alpha_i + \dot{\alpha}_i}{s^2 + bs + k} + \frac{C_0\Delta\delta_{e_i} + (\Delta M_0/I_y)_i}{s(s^2 + bs + k)} + \frac{C_0\dot{\delta}_e}{s^2(s^2 + bs + k)} \quad (B6)$$

and

$$\dot{\alpha}(s) = \frac{(s + b)\Delta\alpha_i s + \dot{\alpha}_i s}{s^2 + bs + k} + \frac{C_0\Delta\delta_{e_i} + (\Delta M_0/I_y)_i}{s^2 + bs + k} + \frac{C_0\dot{\delta}_e}{s(s^2 + bs + k)} \quad (B7)$$

The  $b$ ,  $k$ ,  $\Delta\alpha_i$ , and  $\dot{\alpha}_i$  values are appropriate to the particular linear segment of pitching-moment curve being considered. The term  $C_0\Delta\delta_{e_i}$  is proportional to the change in pitching moment due to elevator deflection from the start of the maneuver ( $\Delta\alpha = 0$ ;  $t = 0$ ) to the beginning of the  $i$ th time interval. The airplane response in the time plane (inverse transformation of eqs. (B6) and (B7)) may be readily evaluated by Heavisides' partial fractions expansion. (See ref. 10.)

To illustrate the use of the Laplace transform method for computing airplane response in pitch-up maneuvers, a sample set of computations is presented for the example airplane at 35,000 feet using the longitudinal control input shown in figure 14 for an initial value  $\dot{n}$  of 0.2 g per second. This control input is slightly different from the corresponding one used in the REAC analysis because of a slightly different initial pitching-moment slope. (See fig. 13.) The pertinent basic data used are given in table IV and in figure 13.

For region I, which corresponds to the linear pitching-moment segment between values of  $\Delta\alpha$  of 0 and 0.0445 (fig. 13),

$$\Delta\alpha(s) = \frac{C_0 \delta e}{s^2(s^2 + bs + k)} = \frac{0.195}{s^2(s^2 + 2.2s + 28.6)} \quad (B8)$$

and

$$\dot{\alpha}(s) = \frac{0.195}{s(s^2 + 2.2s + 28.6)} \quad (B9)$$

The inverse transformations of equations (B8) and (B9) are

$$\Delta\alpha(t) = -0.00052 + 0.00683t + \text{an oscillatory term} \quad (B10)$$

$$\dot{\alpha}(t) = 0.00683 + \text{an oscillatory term} \quad (B11)$$

The oscillatory contributions in equations (B10) and (B11) are generally small and may usually be omitted.

For region II ( $0.0628 > \Delta\alpha > 0.0445$ ),

$$\Delta\alpha(s) = \frac{0.0445s^3 + 0.1048s^2 + 0.490s + 0.195}{s^2(s^2 + 2.2s + 10.7)} \quad (B12)$$

or

$$\Delta\alpha(t) = 0.0422 + 0.0182t + \frac{e^{-1.1t}}{3.085} (0.0071 \cos 3.085t - 0.0089 \sin 3.085t) \quad (B13)$$

and

$$\dot{\alpha}(t) = 0.0182 + \frac{e^{-1.1t}}{3.085} (-0.0353 \cos 3.085t - 0.0121 \sin 3.085t) \quad (B14)$$

For region III ( $0.0768 > \Delta\alpha > 0.0628$ ),

$$\Delta\alpha(s) = \frac{0.0629s^3 + 0.1293s^2 - 0.452s + 0.195}{s^2(s^2 + 1.7s - 8.0)} \quad (B15)$$

or

$$\Delta\alpha(t) = 0.0514 - 0.0244t + 0.0154e^{2.11t} - 0.0038e^{-3.81t} \quad (B16)$$

and

$$\dot{\alpha}(t) = -0.0244 + 0.0325e^{2.11t} + 0.0145e^{-3.81t} \quad (B17)$$

Similarly for region IV, which corresponds to the linear segment of pitching-moment curve between values of  $\Delta\alpha$  of 0.0768 and 0.21 (limit of  $\Delta C_m(\alpha)$  and  $\Delta C_N(\alpha)$  curves),

$$\Delta\alpha(s) = \frac{0.0767s^3 + 0.1849s^2 - 0.264s + 0.195}{s^2(s^2 + 1.7s - 6.6)} \quad (B18)$$

or

$$\Delta\alpha(t) = 0.0323 - 0.0296t + 0.0447e^{1.86t} + 0.0002e^{-3.56t} \quad (B19)$$

and

$$\dot{\alpha}(t) = -0.0296 + 0.0832e^{1.86t} - 0.0007e^{-3.56t} \quad (B20)$$

At the point in time where corrective control is applied (fig. 14) the terms in the numerator of equation (B18) will change (since the initial conditions and the elevator ramp rate have changed), but the denominator will remain the same (corrective control applied in region IV in present example) so that for a corrective-control rate of  $10^0$  per second,

$$\Delta\alpha(s) = \frac{0.1148s^3 + 0.3406s^2 - 0.186s - 1.62}{s^2(s^2 + 1.7s - 6.6)} \quad (B21)$$

or

$$\Delta\alpha(t) = 0.091 + 0.2455t - 0.00294e^{1.86t} + 0.0267e^{-3.56t} \quad (B22)$$

and

$$\dot{\alpha}(t) = 0.2455 - 0.00547e^{1.86t} - 0.095e^{-3.56t} \quad (B23)$$

For corrective-control rates of  $20^0$ ,  $45^0$ , and  $75^0$  per second, it is only necessary to substitute respective values of  $C_0\delta_e$  of -3.24, -7.3, and -12.17 for -1.62 in the numerator of equation (B21). The results

of the computations for this case are presented in table V and in figure 14, where they are compared with the corresponding solutions from the REAC. The agreement shown is fairly good, although it is indicated that linearizing the pitching-moment curve results in a slightly lower peak positive pitching acceleration (and therefore lower overshoot in angle of attack) than the values obtained from the REAC solutions.

## REFERENCES

1. Sadoff, Melvin: Summary of the Flight Conditions and Maneuvers in Which Maximum Wing and Tail Loads Were Experienced on a Swept-Wing Fighter Airplane. NACA RM A55A06, 1955.
2. Sadoff, Melvin, Matteson, Frederick H., and Van Dyke, Rudolph D., Jr.: The Effect of Blunt-Trailing-Edge Modifications on the High-Speed Stability and Control Characteristics of a Swept-Wing Fighter Airplane. NACA RM A54C31, 1954.
3. Matteson, Frederick H., and Van Dyke, Rudolph D., Jr.: Flight Investigation of the Effects of Partial-Span Leading-Edge Chord Extension on the Aerodynamic Characteristics of a 35° Swept-Wing Fighter Airplane. NACA RM A54B26, 1954.
4. McFadden, Norman M., and Heinle, Donovan R.: Flight Investigation of the Effects of Horizontal-Tail Height, Moment of Inertia, and Control Effectiveness on the Pitch-Up Characteristics of a Swept-Wing Fighter Airplane at High Subsonic Speeds. NACA RM A54F21, 1955.
5. Campbell, George S., and Weil, Joseph: The Interpretation of Non-linear Pitching Moments in Relation to the Pitch-Up Problem. NACA RM L53I02, 1953.
6. Anon.: Fundamentals of Design of Piloted Aircraft Flight Control Systems. The Human Pilot. BuAer Rep. AE-61-4 vol. 3, Aug. 1954.
7. Anon.: Handbook of Human Engineering Data. Second ed., Office of Naval Research, Navy Dept., SDC-199-1-2, NavExos P-643, 1951.
8. Baxter, B., and Travis, R. C.: The Reaction Time to Vestibular Stimuli. Jour. Experimental Psychology, 1938, vol. 22, pp. 277-282.
9. McFarland, Ross A.: Human Factors in Air Transport Design. McGraw-Hill Book Co., New York, 1946.
10. Churchill, Ruel V.: Modern Operational Mathematics in Engineering. McGraw-Hill Book Co., New York, 1944.

TABLE I.- DESCRIPTION OF EXAMPLE AIRPLANE

Wing	
Total wing area, sq ft . . . . .	287.90
Span, ft . . . . .	37.12
Aspect ratio . . . . .	4.79
Taper ratio . . . . .	0.51
Mean aerodynamic chord, ft . . . . .	8.08
Dihedral angle, deg . . . . .	3.0
Sweepback of 0.25-chord line, deg . . . . .	35.23
Geometric twist, deg . . . . .	2.0
Root airfoil section (normal to 0.25-chord line) . . .	NACA 0012-64 (modified)
Tip airfoil section (normal to 0.25-chord line) . . .	NACA 0011-64 (modified)
Horizontal tail	
Total area, sq ft . . . . .	34.99
Span, ft . . . . .	12.75
Aspect ratio . . . . .	4.65
Taper ratio . . . . .	0.45
Dihedral angle, deg . . . . .	10.0
Mean aerodynamic chord, ft . . . . .	2.89
Sweepback of 0.25-chord line, deg . . . . .	34.59
Airfoil section (parallel to center line) . . . . .	NACA 0010-64
Maximum stabilizer deflection, deg . . . . .	1 up, 10 down
Elevator	
Area, sq ft . . . . .	10.13
Span, each, ft . . . . .	5.77
Maximum deflection, deg . . . . .	35 up, 17.5 down
Boost . . . . .	hydraulic
Horizontal-tail length, ft . . . . .	18.25
Airplane weight, lb . . . . .	12,400
Airplane mass, slugs . . . . .	385
Airplane pitching moment of inertia, slug-ft <sup>2</sup> . . . . .	17,480
Center-of-gravity location, percent $\bar{c}$ . . . . .	22.5

TABLE II.- SUMMARY OF VISUAL REACTION TIME TESTS

Item	Pilot			Engineer		
	A	B	C	A	B	C
Number runs	33	19	22	53	17	19
Mean reaction time, sec	0.343	0.247	0.246	0.325	0.283	0.31
Standard deviation, sec	0.085	0.045	0.048	0.125	0.036	0.117

TABLE III.- SUMMARY OF PITCHING-ACCELERATION-THRESHOLD TESTS

Item	Pilot			Engineer
	A	B	C	B
Number runs	20	30	19	22
Mean pitching-acceleration threshold, radians/sec <sup>2</sup>	0.093	0.143	0.120	0.124
Standard deviation radians/sec <sup>2</sup>	0.046	0.090	0.072	0.055

TABLE IV.- PERTINENT AERODYNAMIC DATA USED IN ANALYSIS

Airplane lift curve, $\Delta C_N(\alpha)$ . . . . .	See fig. 13
Airplane moment curve, $\Delta C_m(\alpha)$ . . . . .	See fig. 13
Horizontal-tail lift-curve slope, $(C_{L\alpha})_t$ , per radian. . . . .	3.0
Elevator moment effectiveness, $C_{m\delta_e}$ , per radian . . . . .	-0.246
Downwash factor, $\partial\epsilon/\partial\alpha$ . . . . .	See fig. 13
Ratio of horizontal tail to wing dynamic pressure, $q_t/q$ . . . . .	Assumed 1.0
Damping ratio of airplane to that of horizontal tail, K . . . . .	Assumed 1.25
Pressure altitude, $h_p$ , ft . . . . .	35,000
Airplane velocity, V, ft/sec. . . . .	875
Mach number . . . . .	0.90
Mass density of air, $\rho$ , slugs/cu ft . . . . .	0.000736

TABLE V.- SAMPLE COMPUTATIONS

①	②	③	④	⑤	⑥	⑦	⑧	⑨
t	$\Delta\alpha$	$\dot{\alpha}$	<sup>a</sup> $\ddot{\alpha}$	<sup>b</sup> $\frac{-Z_{\alpha}}{mV} \dot{\alpha}$	$\ddot{\theta}$ ④ + ⑤	n	$\Delta L_t \ddot{\theta}$ ⑥ $\times \frac{I_y}{I_t}$	Control rate
0	0	0	0	0	0	0	0	
6.6	.0445	.00683	0	.007	.007	2.29	-7	Entry -1.21°/sec
7.75	.0629	.0223	-.008	.023	.015	2.68	-14	
8.5	.0767	.0545	.146	.024	<sup>c</sup> .170	2.94	-163	
8.55	.1148	.1454	.324	.063	.387	3.46	-370	
8.75	.153	.191	.175	.083	.258	3.93	-250	Recovery
9.15	<sup>d</sup> .232	.218	0	.095	.095	4.90	-90	10°/sec
8.75	.148	.161	-.131	.070	-.061	3.86	60	Recovery 20°/sec
9.15	.181	-.040	-.87	-.02	-.890	4.27	850	
9.35	.152	-.261	-1.33	-.11	-1.440	3.92	1380	
9.54	.0785	-.564	-1.92	-.24	-2.160	2.51	2070	
9.565	.0631	-.613	-2.04	-.27	<sup>e</sup> -2.31	2.47	2220	
9.585	.0534	-.645	-1.63	-.67	-2.30	2.38	2200	
8.75	.143	.087	-.850	.038	-.812	3.80	777	Recovery 45°/sec
8.95	.134	-.192	-1.900	-.080	-1.980	3.70	1890	
9.114	.074	-.576	-2.840	-.250	<sup>f</sup> -3.090	2.88	2960	
8.75	.138	-.003	-1.711	0	-1.711	3.74	1640	Recovery 75°/sec
8.85	.126	-.221	-2.640	-.096	-2.736	3.59	2620	
8.889	.114	-.333	-2.997	-.144	<sup>f</sup> -3.141	3.46	3015	

<sup>a</sup>Obtained by solving equation (B5).

<sup>b</sup> $Z_{\alpha}$  appropriate to linear pitching-moment segment under consideration.

<sup>c</sup>Threshold  $\Delta\ddot{\theta}$  of 0.15 reached.

<sup>d</sup> $\Delta\alpha >$  limit of  $\Delta C_N(\alpha)$  and  $\Delta C_m(\alpha)$  curves.

<sup>e</sup>Peak negative  $\ddot{\theta}$  attained.

<sup>f</sup>Peak negative  $\ddot{\theta}$  reached at maximum available down-elevator deflection.







A-15004

Figure 1.- The example swept-wing airplane.

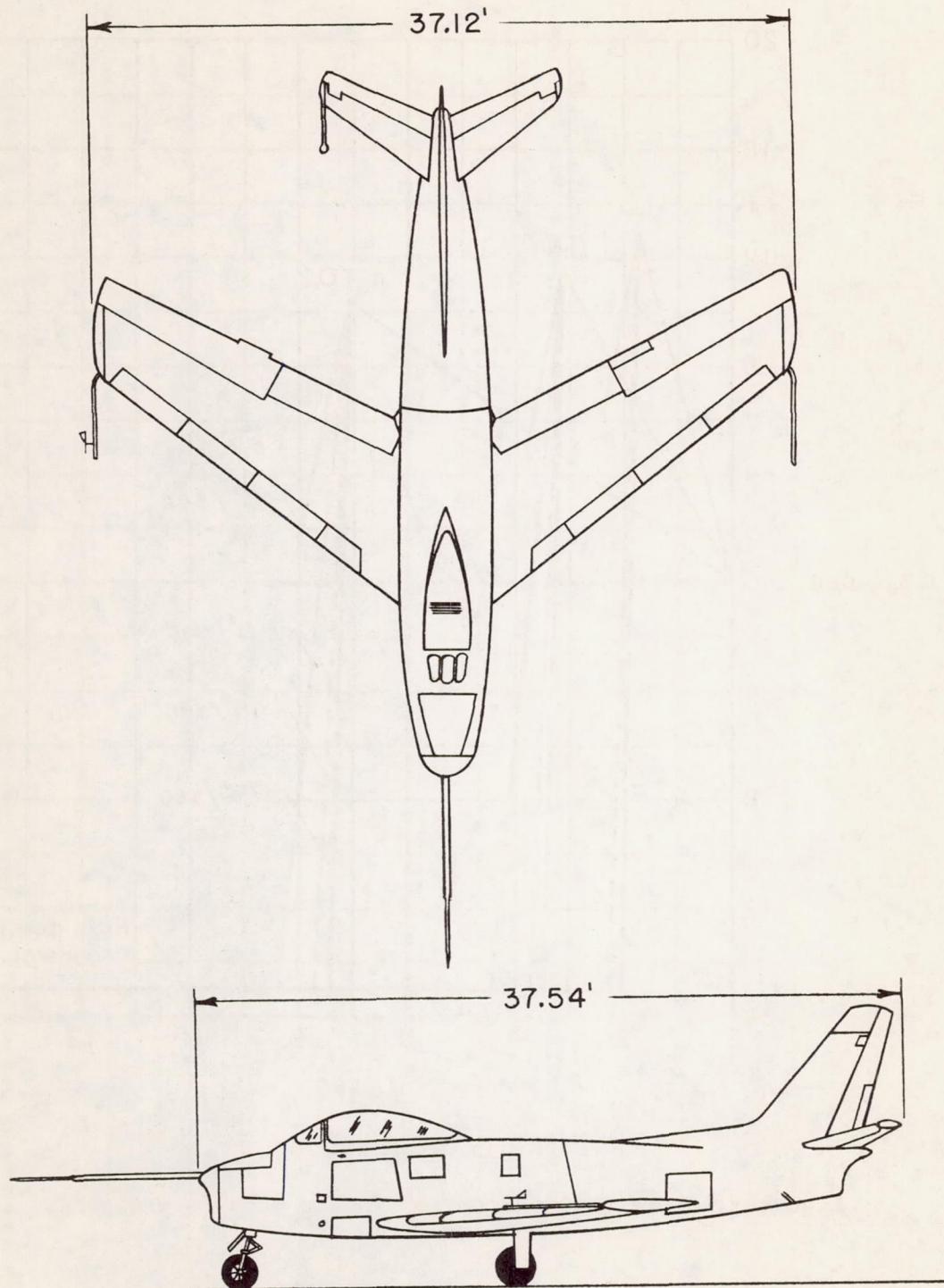
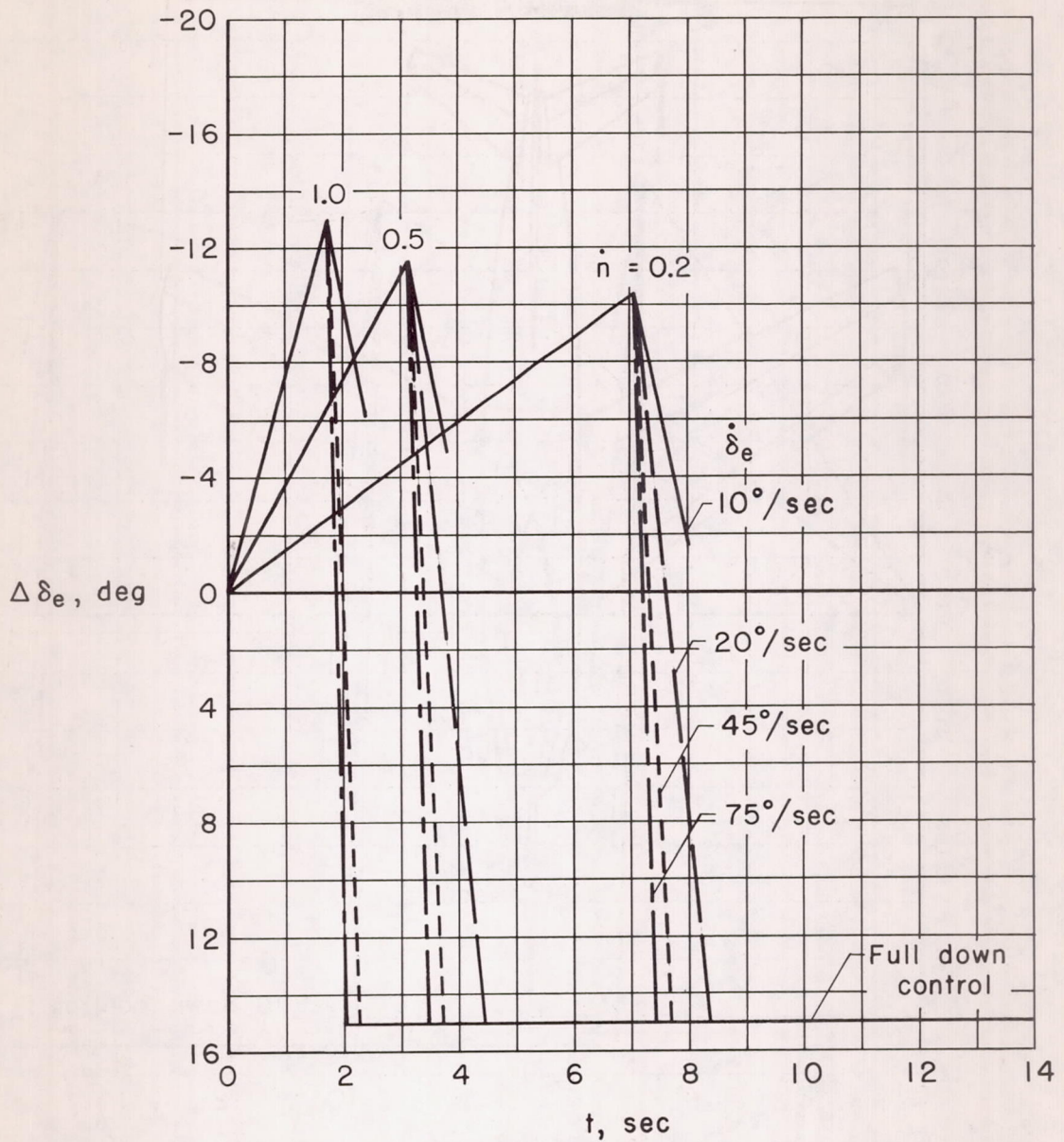
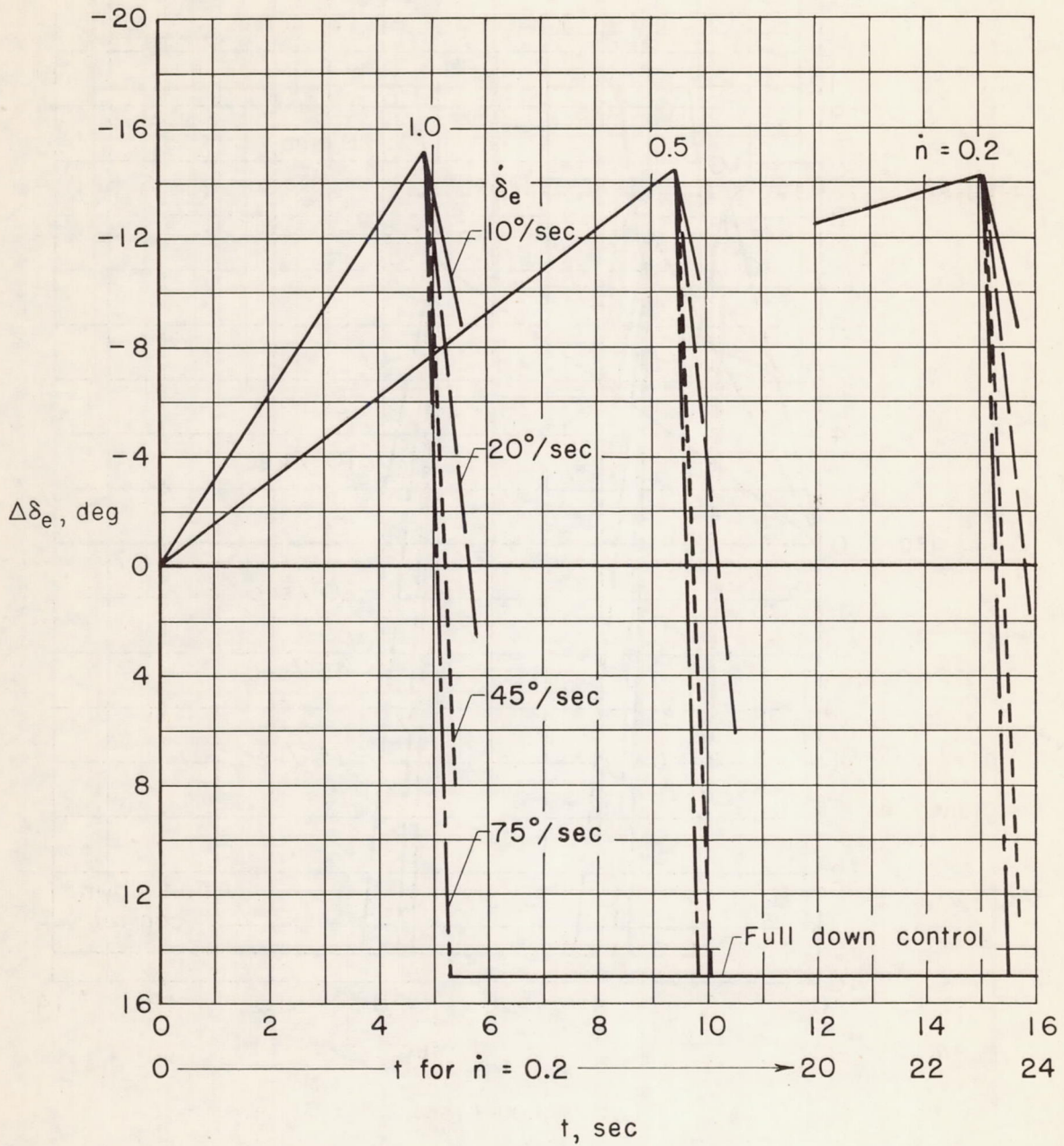


Figure 2.- Two-view drawing of the example swept-wing airplane.



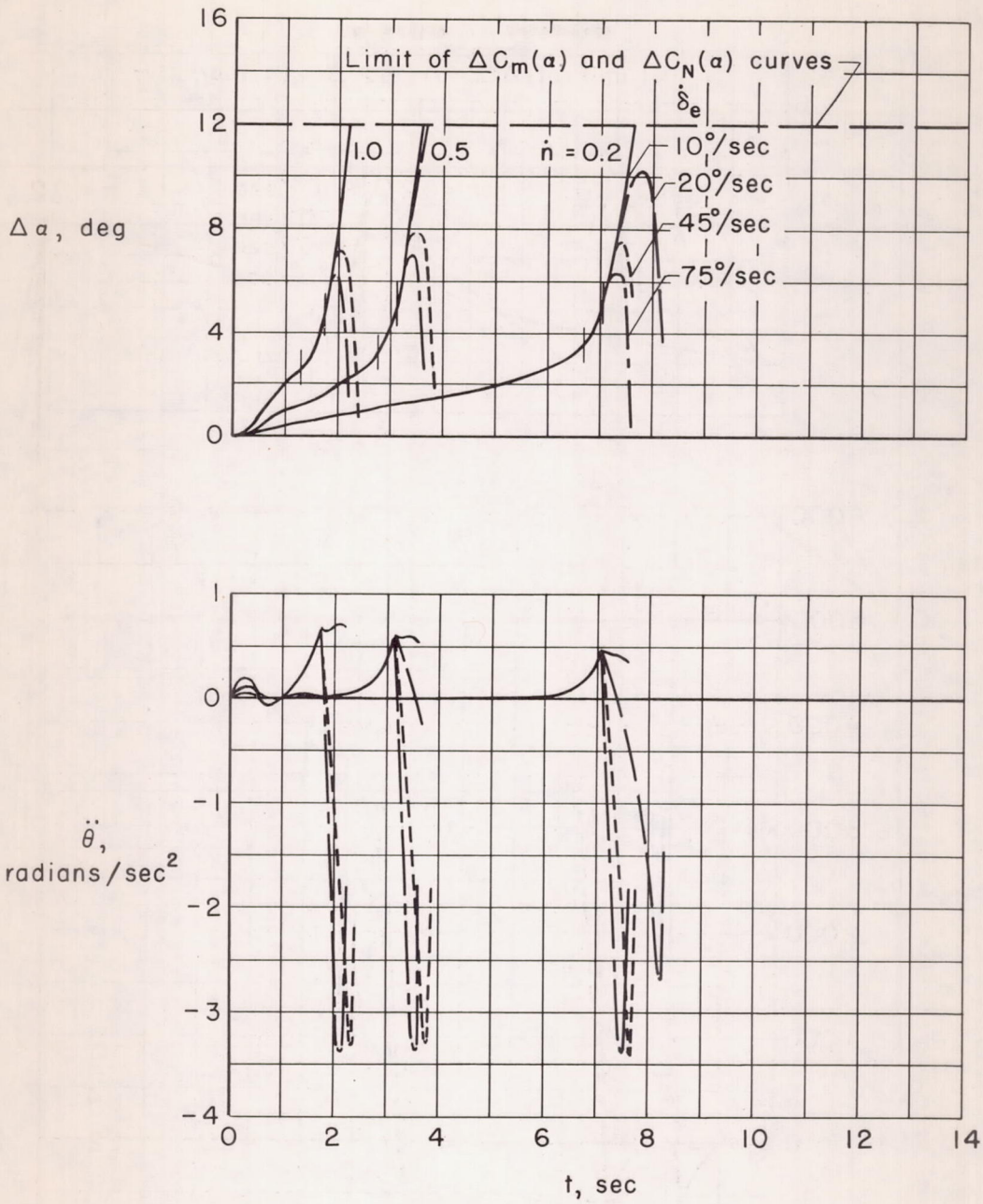
(a) 35,000 feet.

Figure 3.- Longitudinal-control inputs used in analysis.



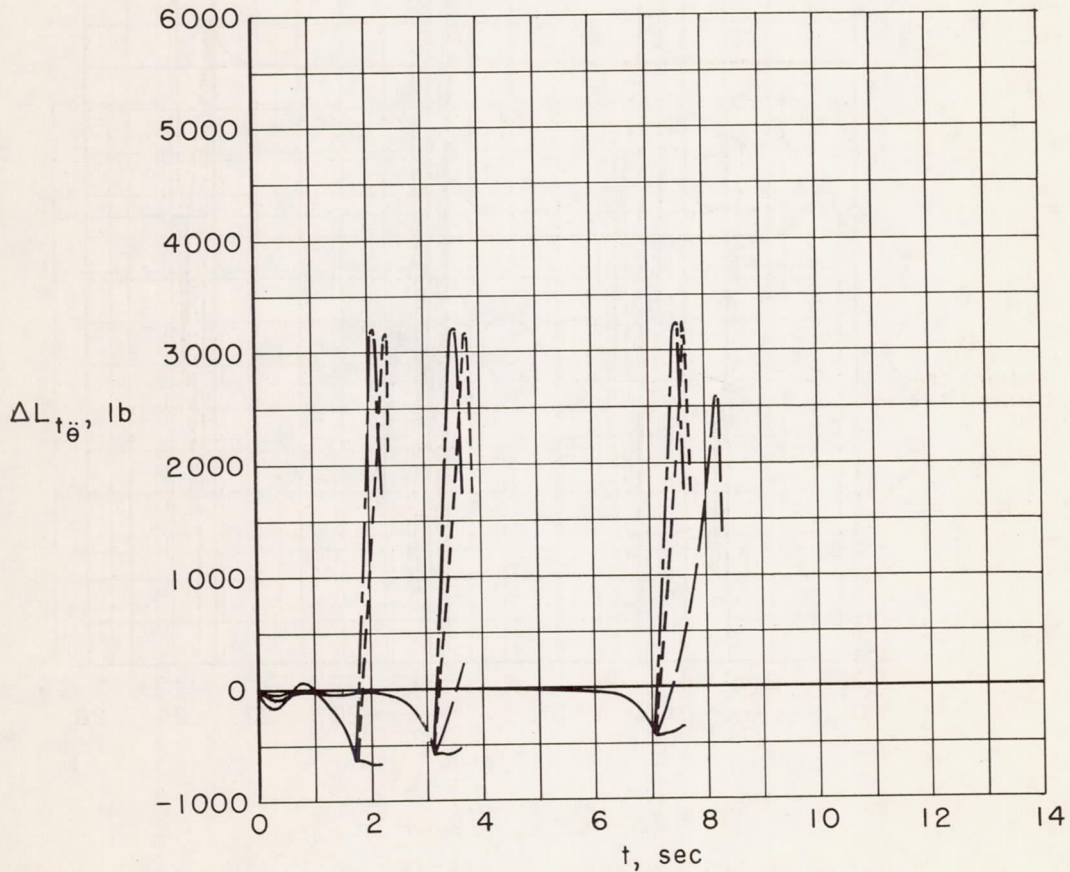
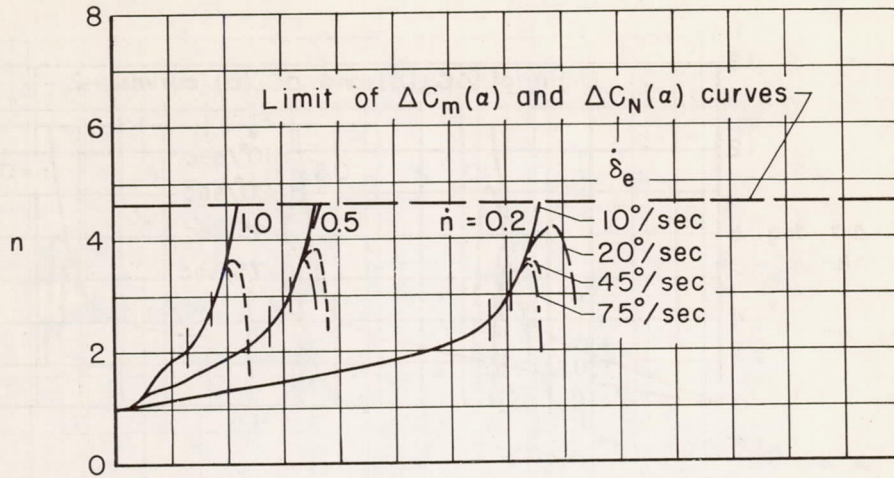
(b) 15,200 feet.

Figure 3.- Concluded.



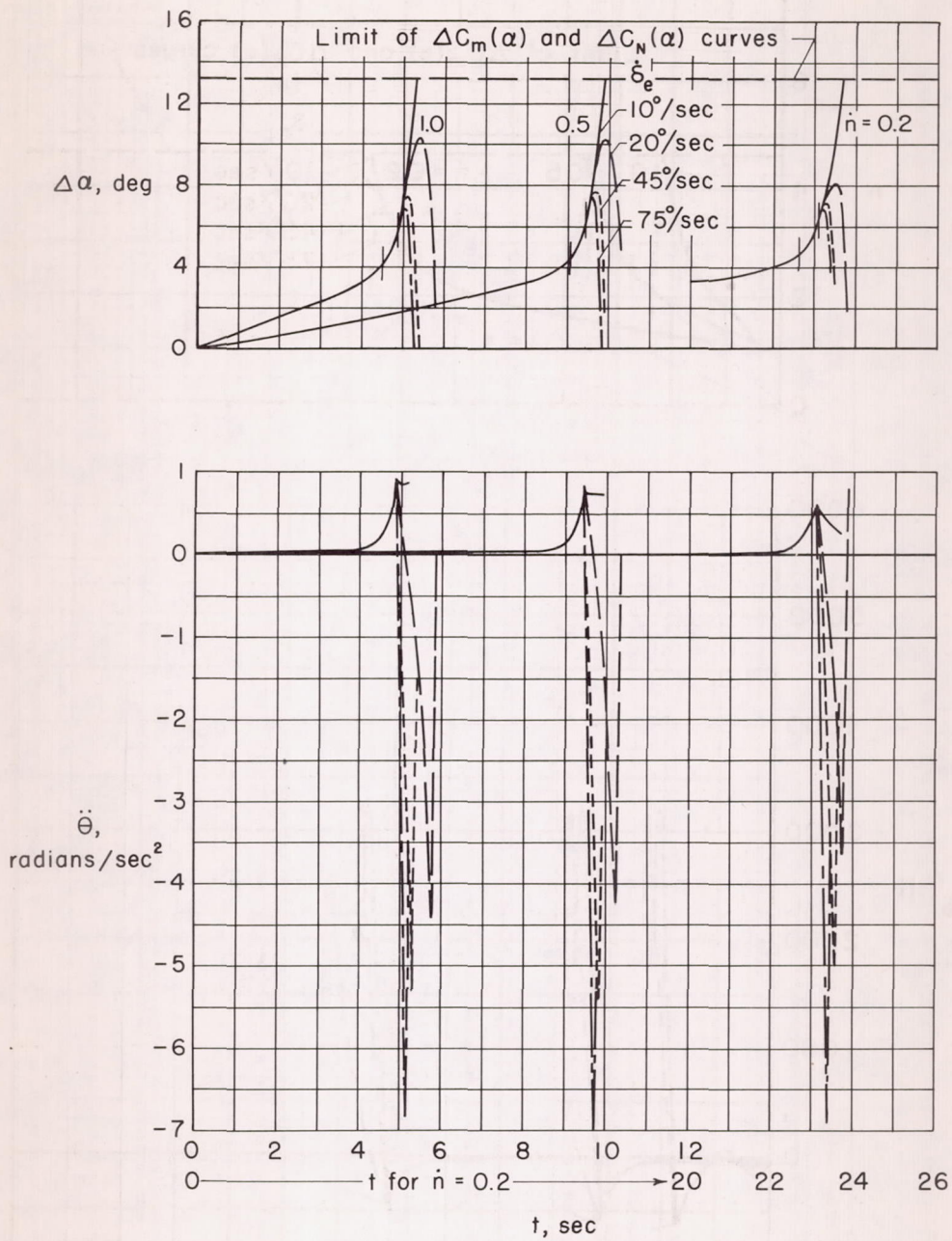
(a)  $\Delta\alpha$  and  $\ddot{\theta}$ .

Figure 4.- Computed response quantities at 35,000 feet.



(b)  $n$  and  $\Delta L_{t\theta}$ .

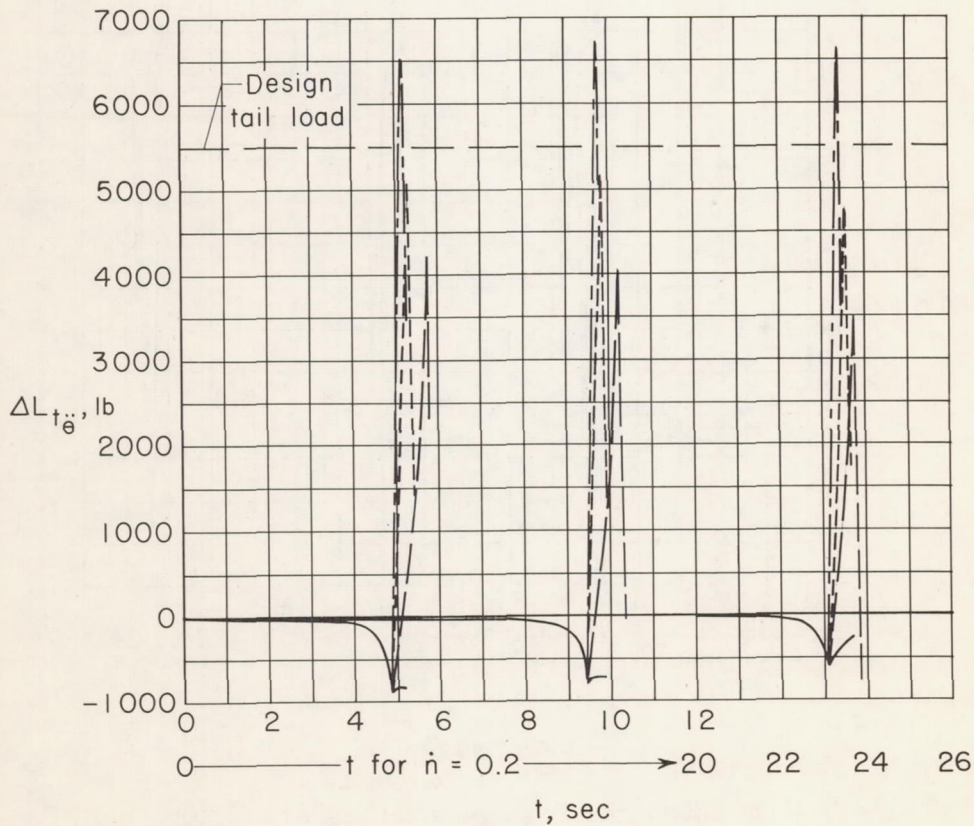
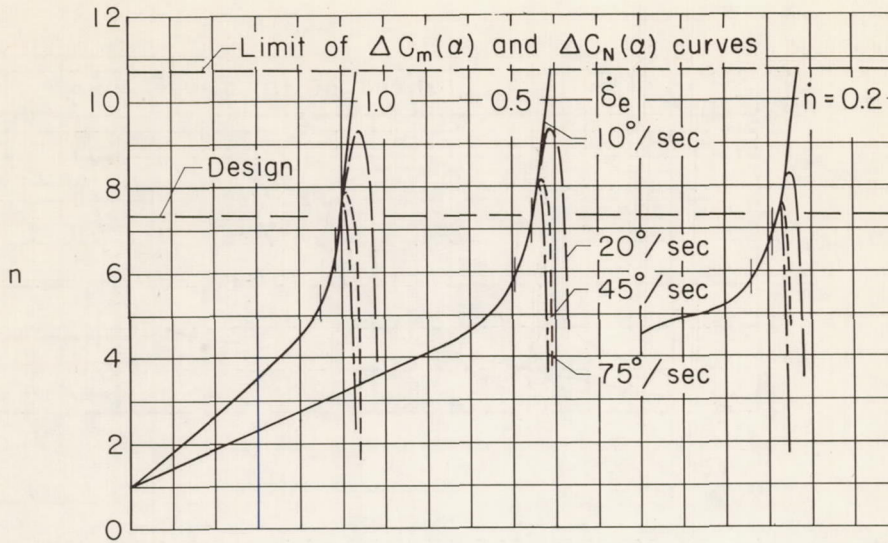
Figure 4.- Concluded.



(a)  $\Delta\alpha$  and  $\ddot{\theta}$ .

Figure 5.- Computed response quantities at 15,200 feet.





(b)  $n$  and  $\Delta L_{t\ddot{\theta}}$

Figure 5.- Concluded.

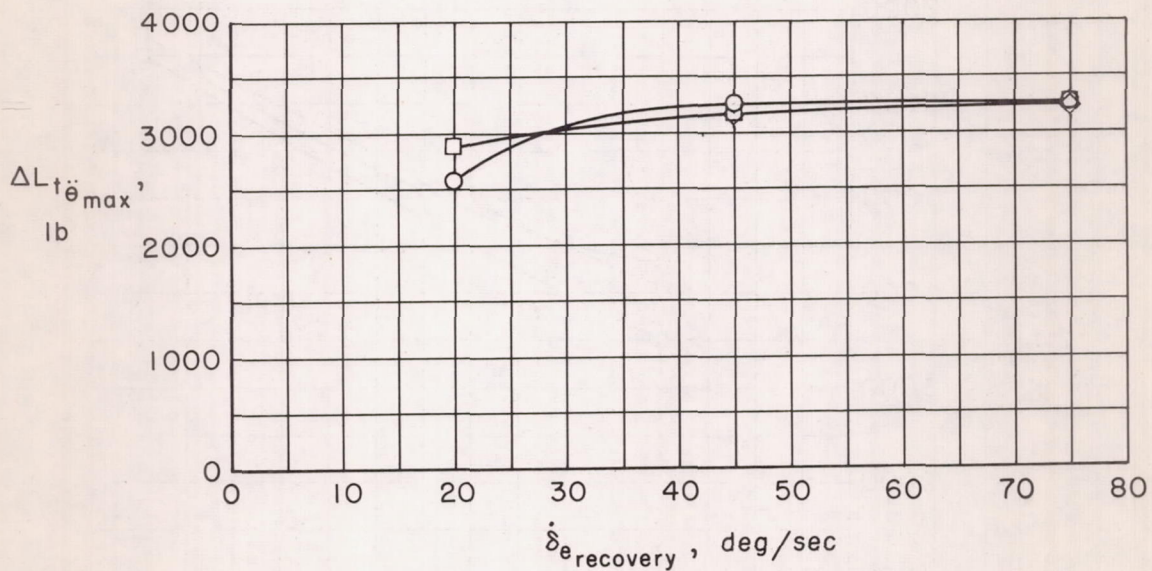
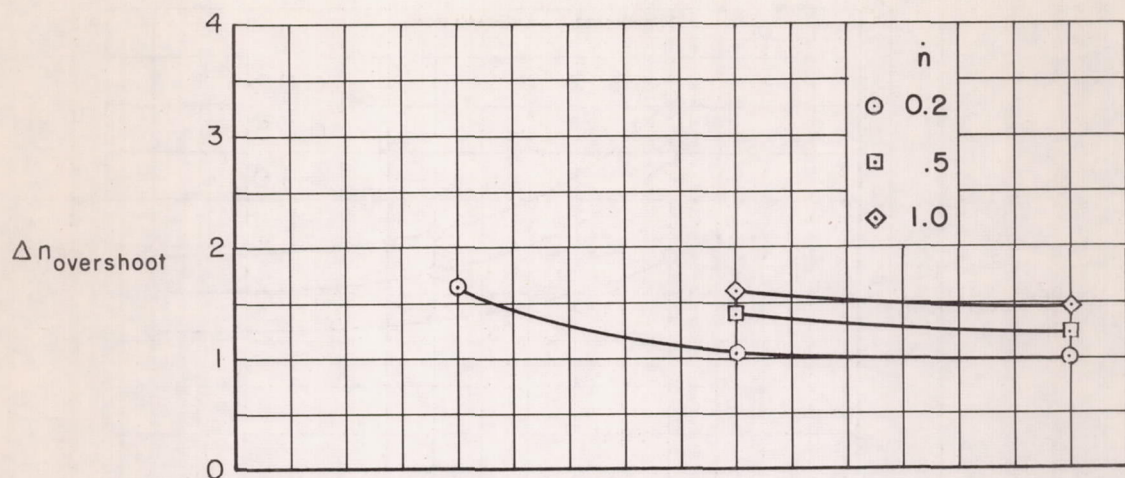


Figure 6.- Variation of overshoot load factor and peak incremental horizontal-tail load with elevator-control rate used in recovery at 35,000 feet.

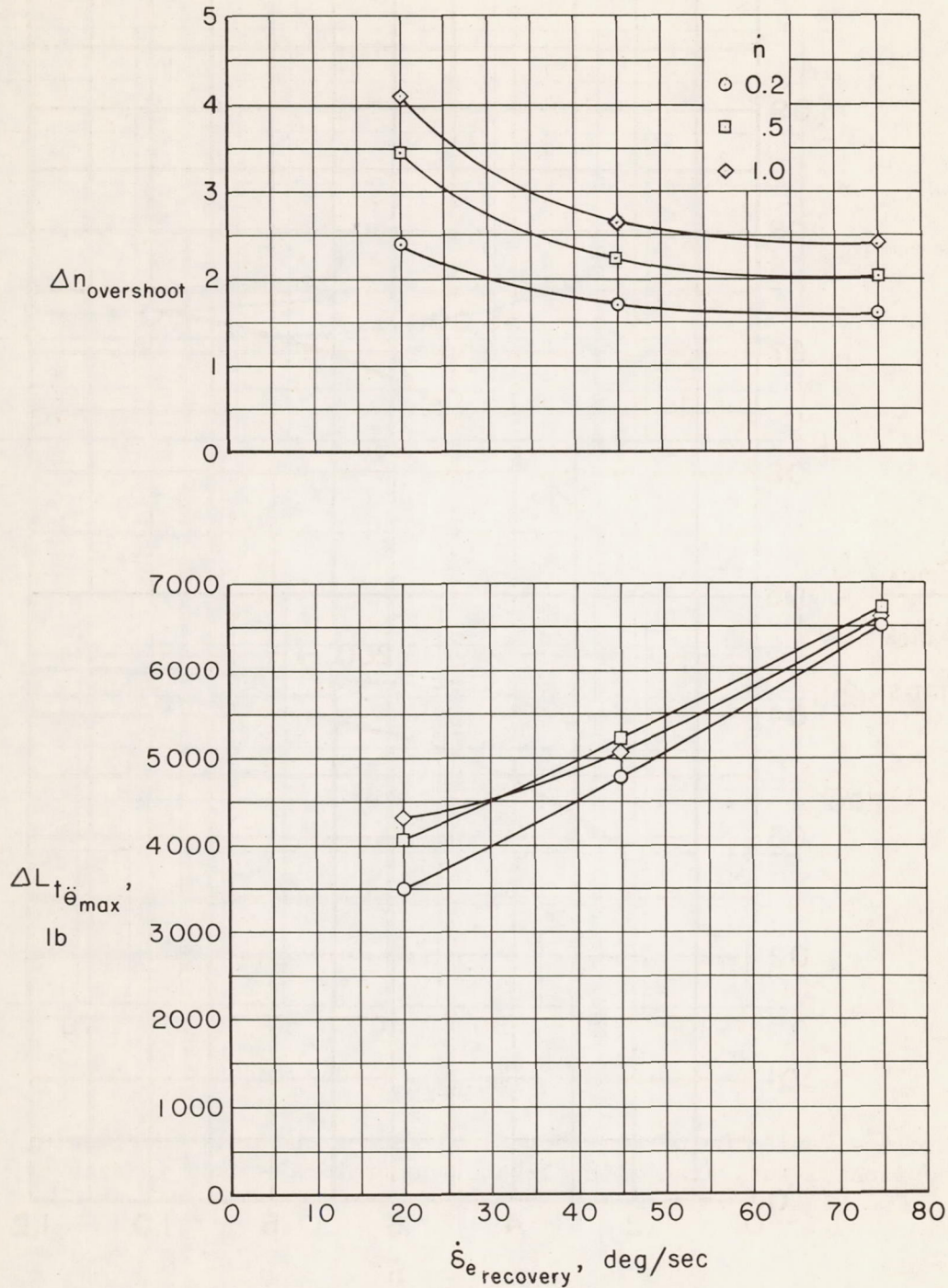


Figure 7.- Variation of overshoot load factor and peak incremental horizontal-tail load with elevator-control rate used during recovery at 15,200 feet.

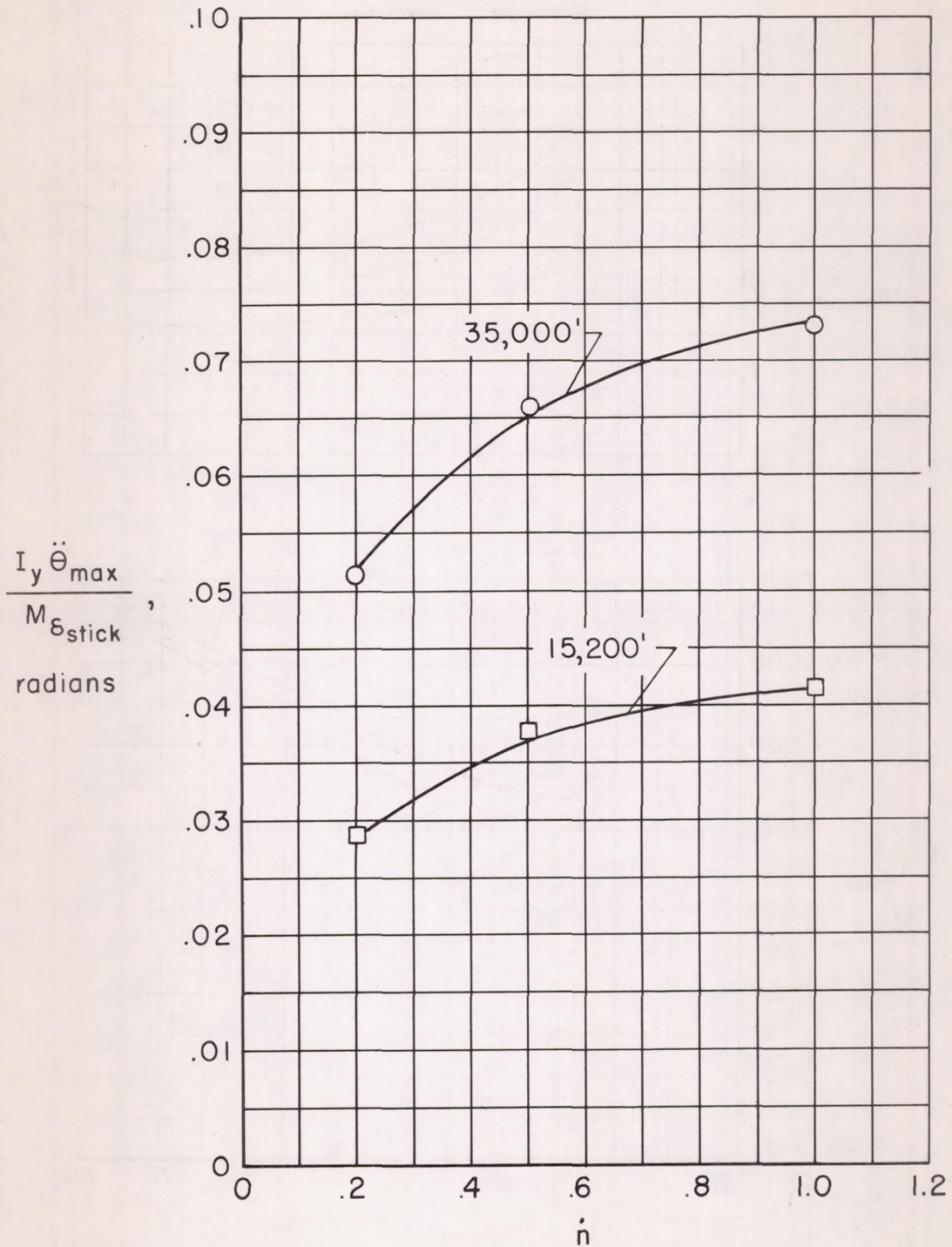


Figure 8.- Variation of controllability parameter  $I_y \ddot{\theta}_{max} / M_{\delta_{stick}}$  with entry rate  $\dot{n}$  at 35,000 feet and 15,200 feet.

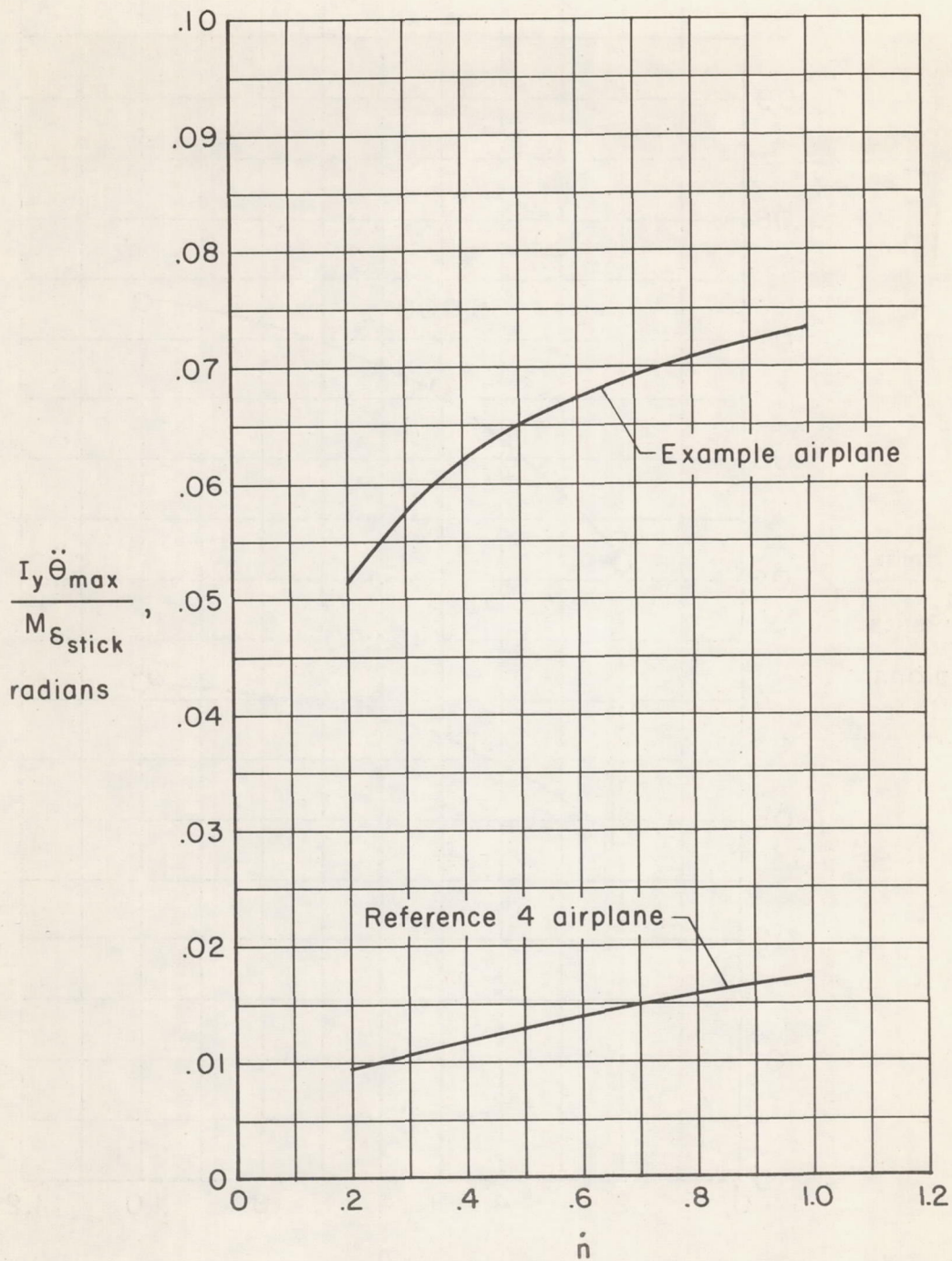
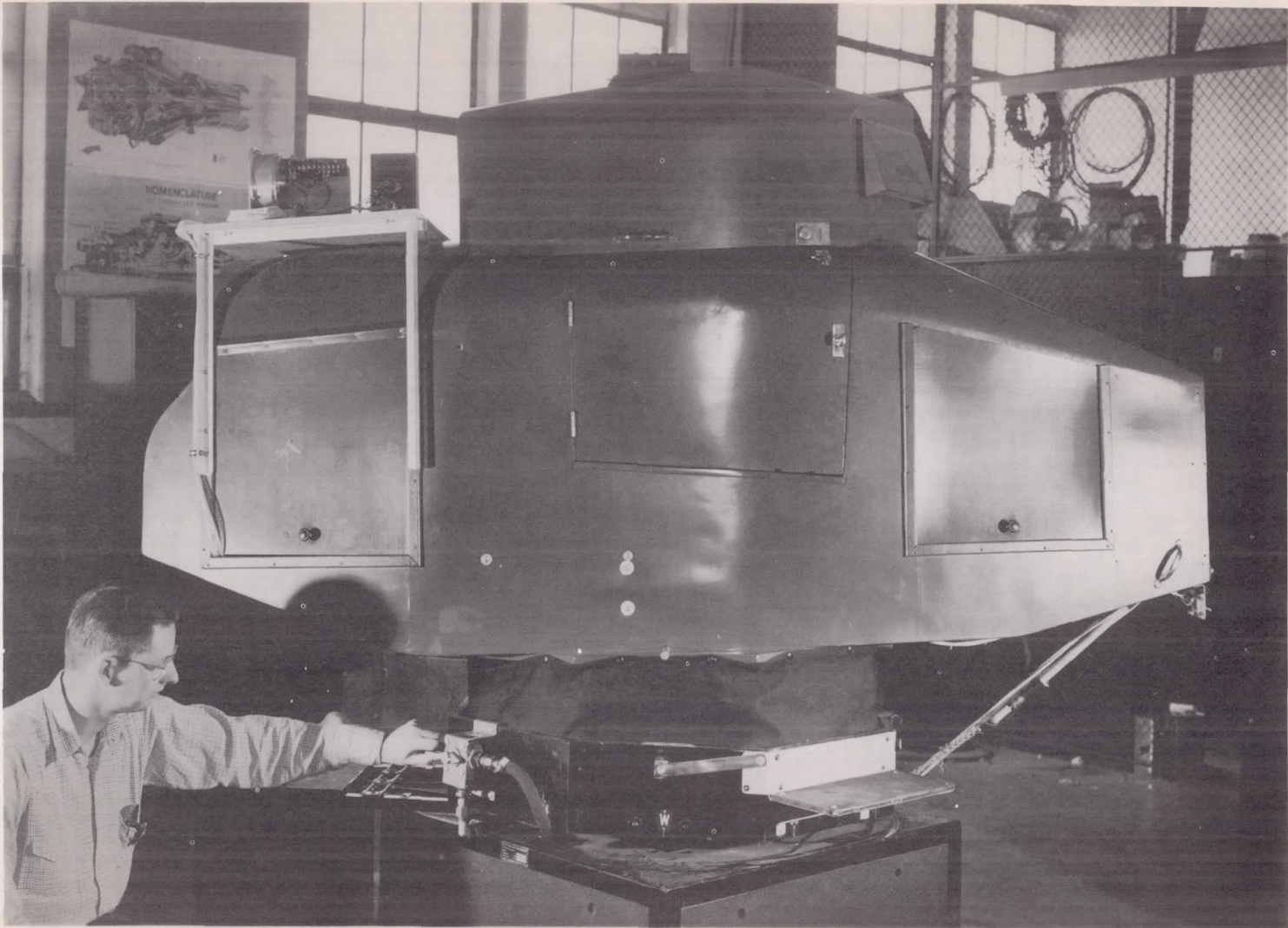


Figure 9.- Comparison between the controllability factors for the elevator-controlled example airplane with those for a similar stabilizer-controlled airplane at 35,000 feet.



CONFIDENTIAL

A-19273

Figure 10.- The modified Link trainer used in response-time and pitching-acceleration-threshold tests.

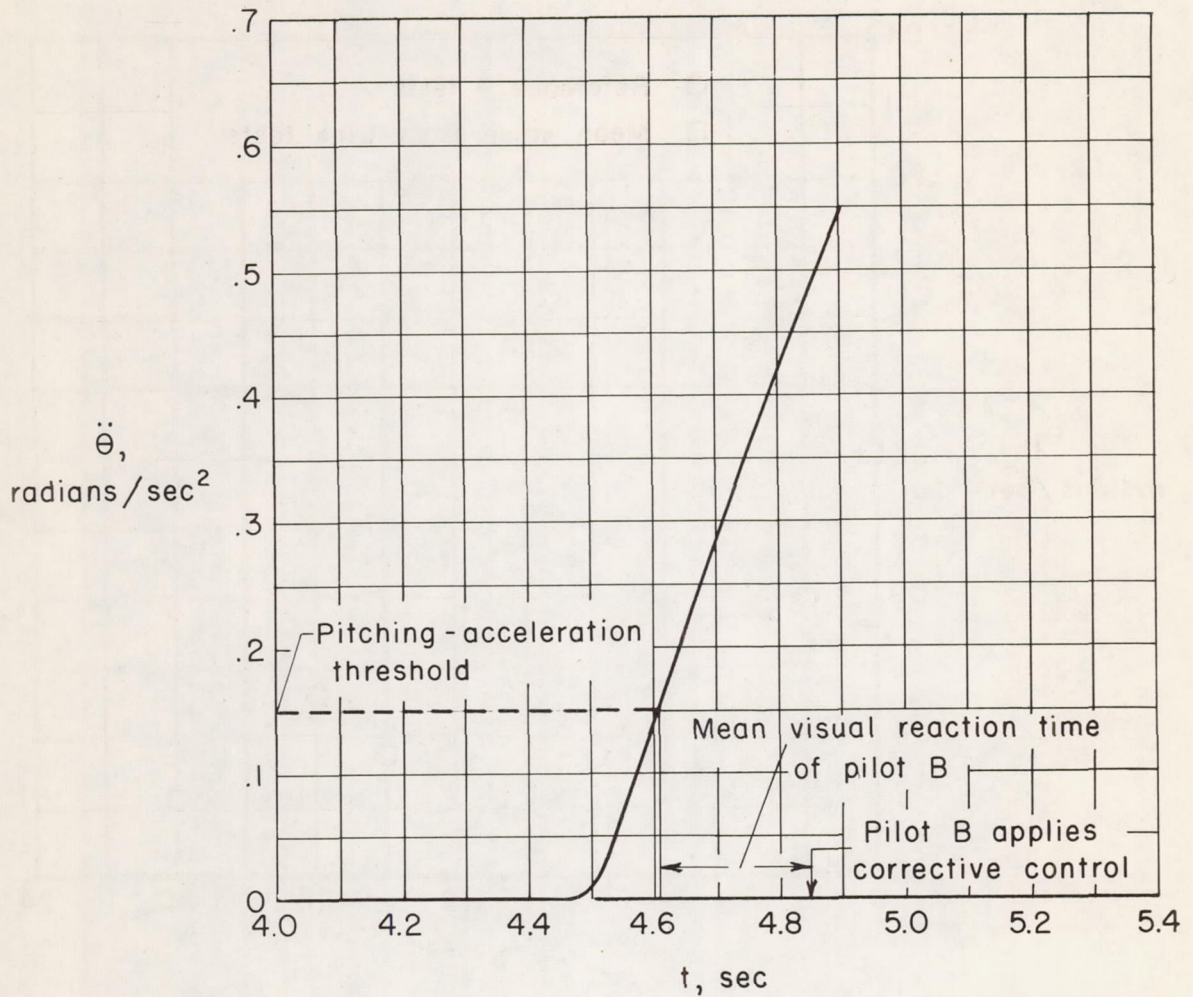


Figure 11.- Procedure used to determine pitching-acceleration threshold.

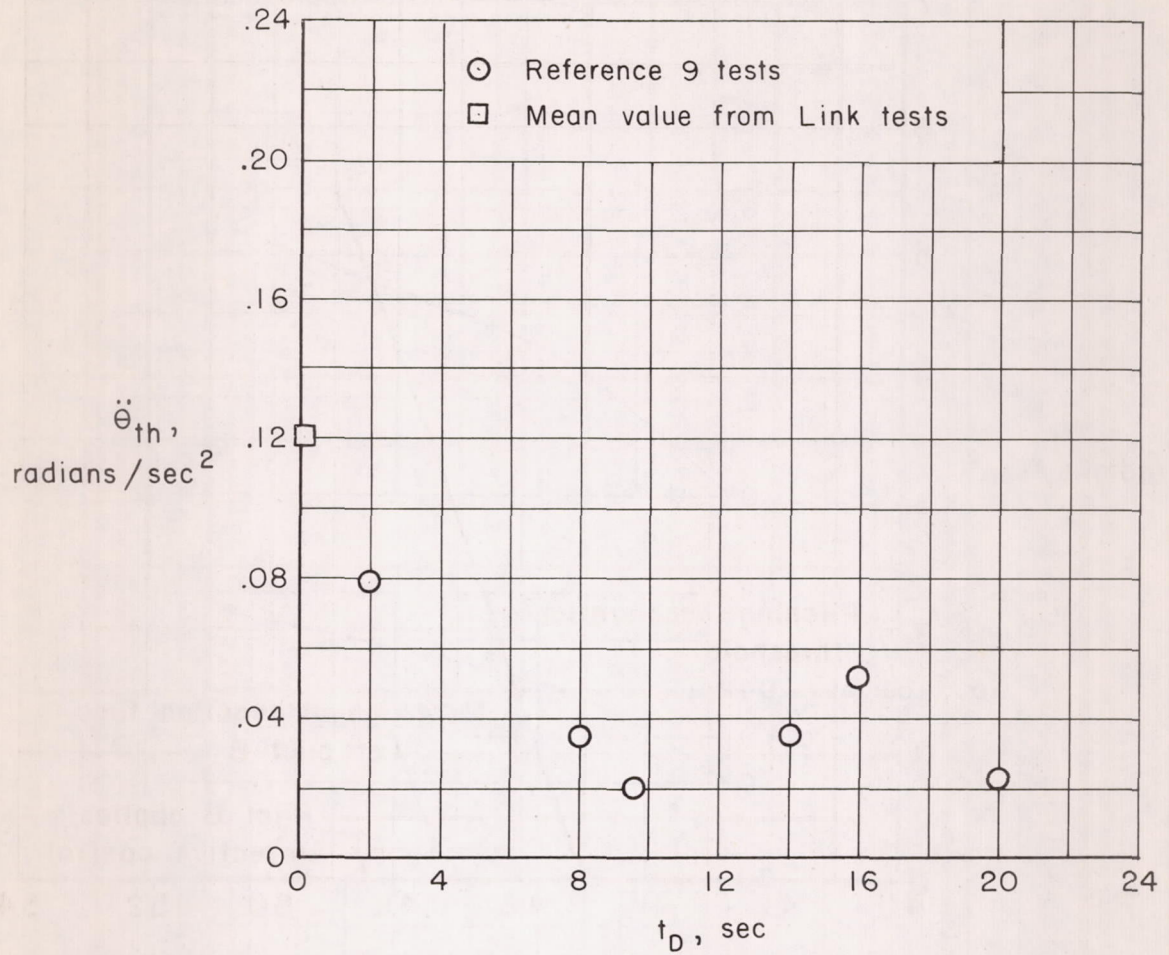


Figure 12.- Pitching-acceleration thresholds from present tests and from tests of reference 9.



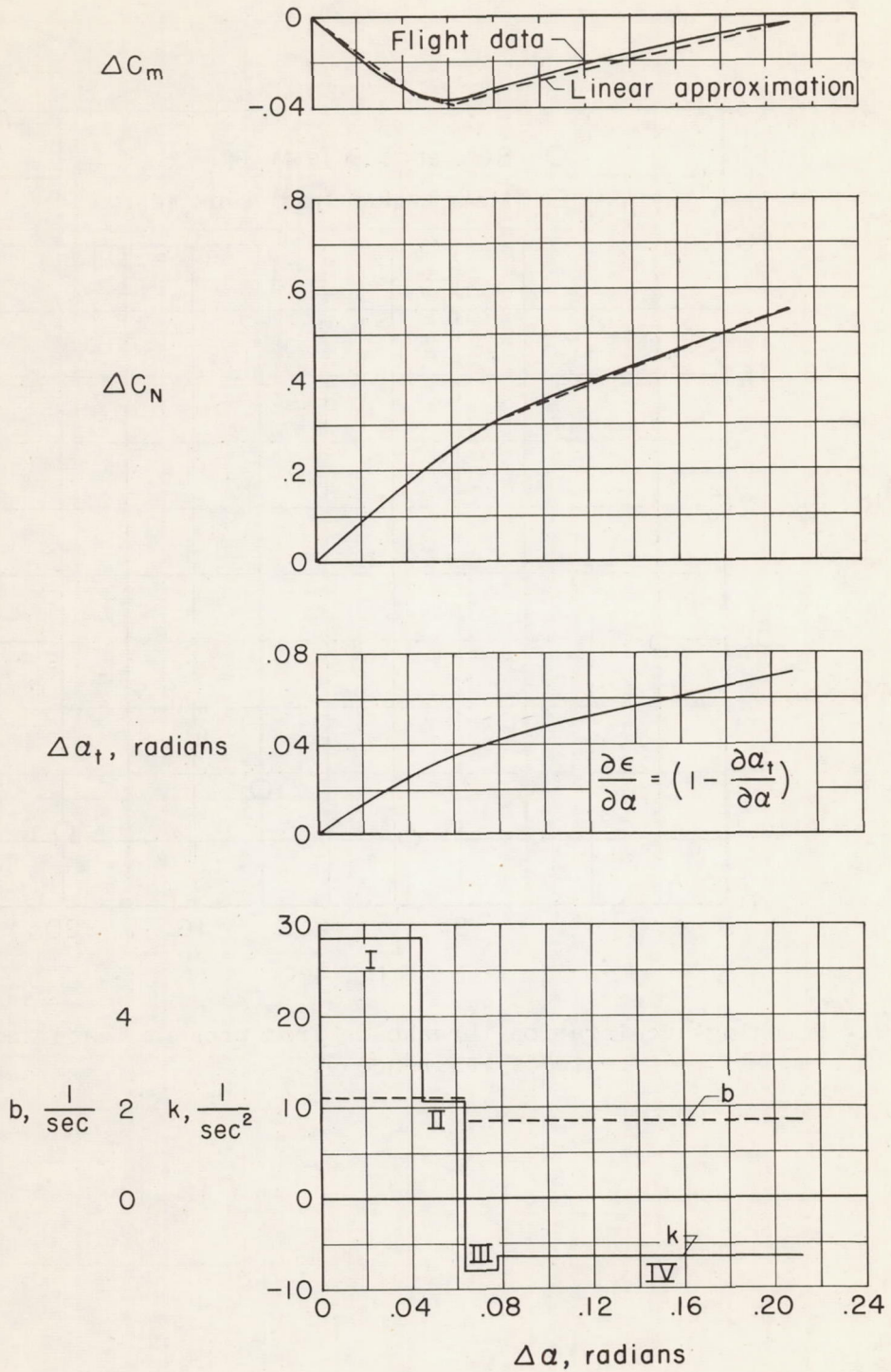


Figure 13.- Pertinent basic data used in analysis; pressure altitude, 35,000 feet.

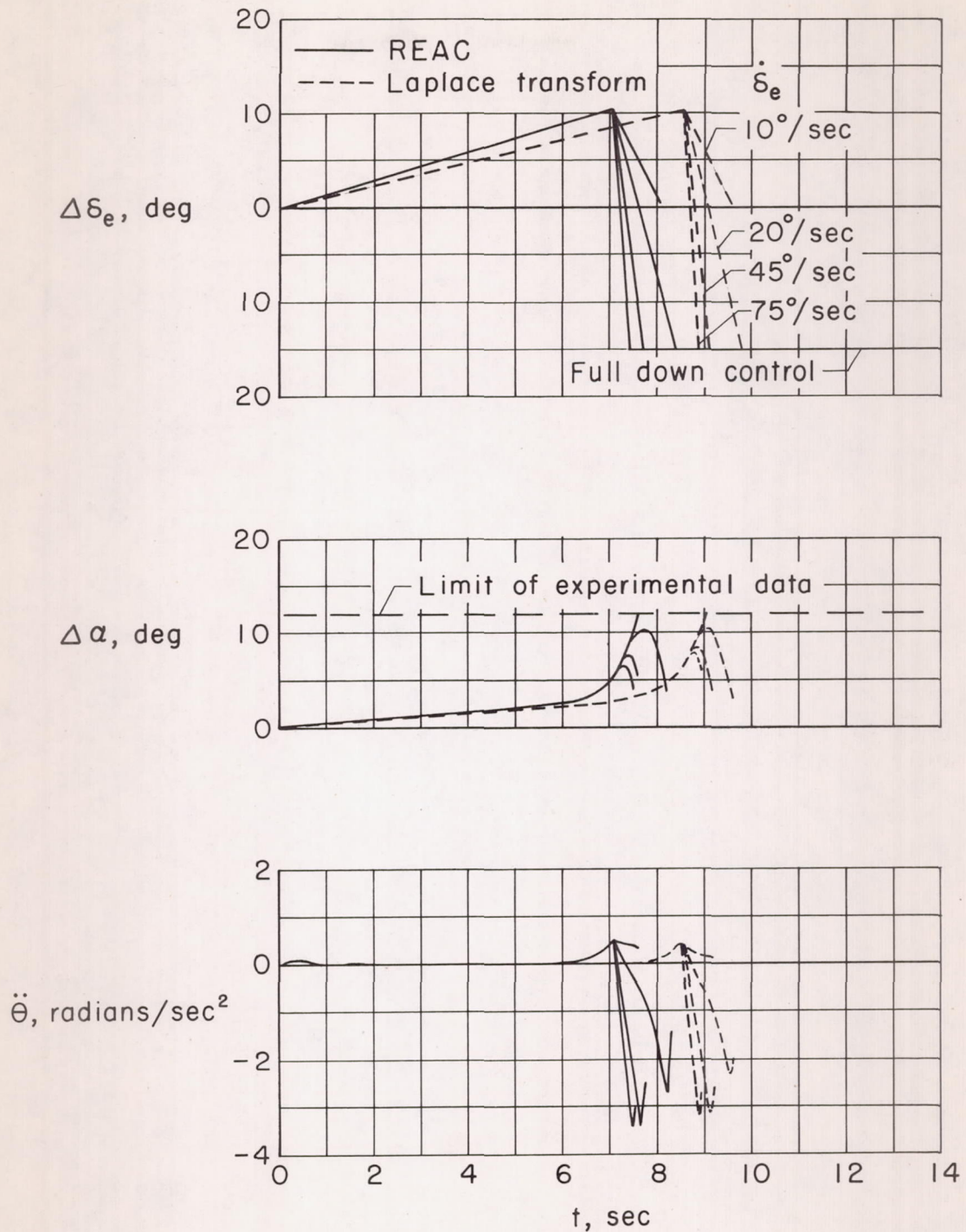


Figure 14.- Comparison of the angle-of-attack and pitching-acceleration responses obtained from the REAC and by the Laplace transform method.

**CONFIDENTIAL**

**CONFIDENTIAL**